24th COBEM - 2017

24th ABCM International Congress of Mechanical Engineering
December 3-8, 2017, Curitiba, PR, Brazil

COBEM-2017-0948
NUMERICAL SIMULATION OF AN EJECTOR USING THE OPENFOAM® SOLVERS

Wellorzzon Ronnan Ibide Novais
Vicente Luiz Scalon
São Paulo State University (UNESP), School of Engineering, Bauru, Brazil
well.orz.zon@gmail.com, scalon@feb.unesp.br

Abstract: *A new researching technology can use the Sun heat energy to complete the refrigeration cycle without the compressor, the most power consumer device in an air conditioner. It can be achieved replacing the compressor by an ejector, however, it results in a lower performance of the system, which can be improved increasing the ejector's performance using the CFD simulations. In this work the CFD software OpenFOAM was used to validate the model that will be used to perform a future performance analysis of an ejector. The solvers rhoCentralFoam, rhoPimpleFoam, sonicFoam and modFoam, a new solver created to enable Peng-Robinson gas equation, were analyzed with an initial mesh of about 11.000 quadrangular cells and the standard* $k - \epsilon$ *turbulence model. The lab conditions and results were based on a previous work performed with the R-134a refrigerant fluid. The solvers rhoPimpleFoam and rhoCentralFoam were unfeasible due to high time requirement or instability. The ratio between the input mass fluxes were better predicted by the sonicFoam, while the wall pressure in the mixing chamber had better results using the modFoam. The initial mesh presented good accuracy, but future analysis are required to understand why the mesh refinement influenced negatively on the accuracy.*

Keywords: *ejector, OpenFOAM, air conditioner, sonicFoam, rhoCentralFoam*

1. INTRODUCTION

By the end of the 20th century the global warming started to take the attention on the scientific community. The greenhouse gases level was continuously growing exceeding the historical confirmed amount related to the time where there was no industrialization. Currently the burning amount of fuels to generate electrical energy is high and the transition to renewable energy sources is important to decrease the global warming advance.

The increase of global warming and the feasibility to acquire an air conditioner increased the power consumption for environment refrigeration, as a result, the demand for new power sources also increased, mainly in Mexico, Brazil, India and China. As consequence the environment degradation become worst because of the building of new power plants as an emergency action, without planning and based on burning of fossil fuel, or even for the release of more greenhouse gases in the atmosphere for just use more energy. There are some cases, however, that the air conditioner is essential for health purposes, like its relevance when the heat waves hits a place, a common problem in Australia. The installation of air conditioners is the emergency plan, but the high electric power consumption can result in a failure of the power plant in the hotter time.

A solution could be the investment on new technologies to air conditioner system to increase the efficiency and decrease its global warming potential. One of these new technologies is the replacement of all or most part of the electrical power consumed using the solar energy. In this way the space cooling uses the Sun heat energy to complete the refrigeration cycle without the compressor, currently the most power consumer device in an air conditioner system.

The ejector is the main device in this solar refrigeration system and it will always be attached to a hot source, like solar thermal collector (the generator, or energy source). The air conditioner system works, basically, as shown by the Fig. 1a and the ejector internal process can be followed in the Fig. 1b. The steps of the entire refrigeration cycle can be divided and described like below:

1. The refrigerant fluid is heated in the generator (solar thermal collector, for example) reaching a high pressure and high temperature.

2. The stream from the generator enters in the ejector as a primary stream and reaches supersonic speed after the nozzle.

3. Then the secondary stream is moved by the movement of the primary one, which is the main effect of the ejector.

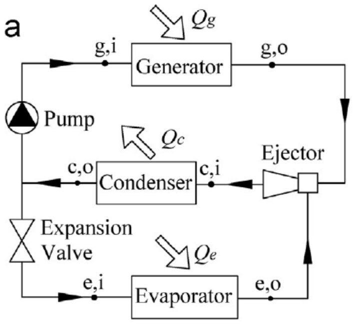

(a) Refrigeration cycle using an ejector
(Source: Ablwaifa, 2006)

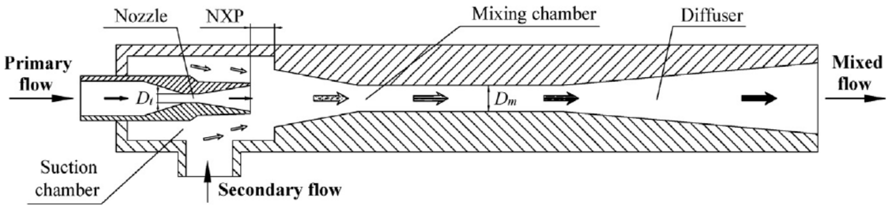

(b) Ejector working principle (Source: Chen *et al.*, 2015)
Figure 1: Details of the refrigeration cycle and ejector

4. In the mixing chamber both streams are mixed and stabilized. During the mixing process, the primary stream pressure decrease, while the secondary stream pressure increase. The effect in the velocity is the opposite, decreasing the primary stream velocity and increasing the secondary one.
5. Finally the mixed stream reach the diffuser, where they low the speed even more and increase the pressure up to acceptable values to enter in the condenser.
6. The mixed stream move forward to be cooled in the condenser. After that the refrigerant fluid is divided again into the same two streams:
   (a) The first one (primary stream) is driven to the generator, however, it needs an auxiliary pump to reach it. This pump can be moved by electrical energy from a photovoltaic system, or even from the common electrical power distribution network.
   (b) The second stream is driven to the expansion valve and then to the evaporator, which will cool the room.

The refrigeration system using solar energy, however, has a low performance compared to the systems using a compressor or absorption cycle, like has been observed by Chen *et al.* (2015). The main reason is the low coefficient of performance from the ejector, which is defined by the Eq. (1). In thermodynamics the Coefficient of Performance (COP) is known as a ratio between the desired effect (the amount of extracted heat from the room) and the required input (amount of absorbed heat by the generator). The need to increase the system performance has moved researchers to find some possible improvements in refrigeration system devices and the relevance of each one of them.

$$COP = \frac{Q_{extracted\ heat}}{Q_{absorved\ heat}} = ER \cdot \frac{\Delta h_{evap}}{\Delta h_{gen}} \tag{1}$$

$$ER = \dot{m}_s / \dot{m}_p \tag{2}$$

where:
ER is the ratio between the mass flux inputs,
Δh_{evap} is the enthalpy variation between the evaporator inlet and outlet,
Δh_{gen} is the enthalpy variation between the generator inlet and outlet,
$\dot{m}_s$ is the secondary mass flux,
$\dot{m}_p$ is the primary mass flux.

One way to improve the performance of this kind of refrigeration system is increasing the ejector COP using aimed studies to the understanding of generated physical effects related to the ejector and how to minimize the losses. Some works have been developed and the trend is the numerical simulation application, which helps the ejector analysis for high performance purposes. Some different softwares have been used, but just a few studies include the OpenFOAM, known as a good software for CFD (Computational Fluid Dynamics) simulations. Among the solvers available in OpenFOAM, there are some that can be used for compressible fluids and trans-sonic/supersonic flow, like the sonicFoam, rhoPimpleFoam and rhoCentralFoam, which will be used in this work.

There are two ways to analyze a device: the lab experiment or the computational one. The first is one of the best ways of researching about what are the effects with big importance and how they behave, but some researching parameters can not be measured in real conditions and the various test modifications demand a long time, as explained by Zikanov (2010, p. 3). The second one is more suitable for the analytical and theory understanding, but Versteeg and Malalasekera (2007, p. 16) have explained that the computational experiment is an affordable analyzing way for the cases with predictable behavior in real conditions, keeping the equipment costs low and an easy changeable process for the project parameters.

There are various analyses for the studied case on which the ejector was investigated in a lab experiment, like the one developed by García del Valle *et al.* (2014), as well as the studies with both lab and computational analysis as those simulated by Bartosiewicz *et al.* (2005); Cardemil and Colle (2012); García del Valle *et al.* (2015). The CFD studies, however, can be divided according to the fluid behavior (single or bi-phase), dimensional planes calculated during the simulation (one, two or three dimensional planes) and also according to the ejector geometry or shape.

Bartosiewicz *et al.* (2005); Hakkaki-Fard *et al.* (2015); Allouche *et al.* (2014) have used as an useful simulation technique to increase the performance of the ejector the prediction of big characteristics of its behavior as well as the understanding and visualization of internal physical effects, understanding how the shock waves work (the main internal irreversibility), what are its effects in the efficiency decrease and how to minimize them. This type of analysis can be done with just a two-dimensional mesh.

Hakkaki-Fard *et al.* (2015) have demonstrated improvements on the ejector's performance up to 29% related to the inlet mass flux ratio and it can be achieved optimizing the device for a specific working condition. According to Eq. (1) it can be noticed the increasing in the ER is directly proportional to the ejector's COP. Hakkaki-Fard *et al.* (2015) have shown some details that must be observed during the ejector's operation: in the area next to the mixing chamber both streams must flow in parallel, the secondary stream must be near the supersonic speed and the primary flow must be fully expanded or slightly over-expanded. All this information is useful to verify what are unappropriated conditions and what are the dimensions that must be changed to minimize the process irreversibilities.

In the case of the ejector, the computational experiment can be applied because its behavior is predictable and it has many articles already published using lab experiments, like those shown by Yen *et al.* (2013); Abed *et al.* (2016); García del Valle *et al.* (2014), which can be used to verify the effectiveness and accuracy of the computational analysis. A computational analysis for the ejector was developed by García del Valle *et al.* (2015) to verify its previous experimental work. The thermodynamic properties changed from ideal gas to real one directly influenced the pressure and temperature calculation on the numerical simulation, mainly the temperature.The results present the standard $k-\epsilon$ model as the best to define the mixing between the two coaxial streams and to predict the shocking waves position. Finally, for low inlet mass flux ratios an independence between this parameter and the pressure profile in operational conditions has been observed.

2. COMPUTATIONAL PROCEDURE

García del Valle *et al.* (2015) have shown a comparison between the lab and computational experiments, proving that is possible to achieve great precision using the simulations. Their work is the base for the analysis presented here, which is focused on simulating the lab conditions and comparing the results to them. The refrigerant fluid used is the HFC-134a (or R-134a) and initially just the first of the four casessimulated in their work will be simulated in different solvers with an initial test mesh described in the sections below. This initial mesh is used to check the stability and convergence of the solver, which will be achieved modifying some analysis characteristics, like the time step and boundary conditions. The test conditions of the lab experiments are summarized in the work from García del Valle *et al.* (2015).

2.1 The base theory in the CFD softwares

The CFD softwares, in general, work with math equations to solve the cases. Some of the main equations are the mass, momentum and energy conservation. Those equations are described below: the Eq. (3) is the mass conservations equation, the Eq. (4) is the momentum conservation equation and the Eq. (5) is the energy conservation equation in terms of the specific total energy. The energy conservation calculation using the total energy has a great importance, since it has significantly more precision compared to the use of just the thermal energy.

$$\frac{\partial \rho}{\partial t} + \nabla \cdot (\rho \mathbf{U}) = 0 \tag{3}$$

$$\frac{\partial}{\partial t}(\rho\,\mathbf{U}) + \nabla\cdot(\rho\,\mathbf{U}\otimes\mathbf{U}) = -\nabla\cdot p\,\mathbf{I} + \nabla\cdot\boldsymbol{\tau} + \rho\,\mathbf{g} \tag{4}$$

$$\frac{\partial \rho e}{\partial t} + \nabla\cdot[\rho\mathbf{U}e] = -\nabla\cdot\dot{q}_s - \nabla\cdot[p\mathbf{U}] + \nabla\cdot[\tau\cdot\mathbf{U}] + \rho\mathbf{g}\cdot\mathbf{U} + \dot{q}_V \tag{5}$$

where:

e is the specific total energy,
t is the time,
p is the pressure,
U is the flux velocity vectorial field,
ρ is the fluid density,
I is the identity matrix,
τ is the deviatoric stress tensor
g represents body accelerations acting on the continuum, for example gravity, inertial accelerations.

In the fluid dynamics simulations the turbulence flow regime can be obtained by direct numerical simulation (DNS), large eddy simulation (LES) or Reynolds averaged Navier-Stokes equations (RANS). In the engineering field the DNS and LES models has a limited application to require a very refined mesh and little time steps, which results in high computational costs with resources and time. The CFD simulations using the RANS model has the turbulence flux based on the averaged time solution of the Navier-Stokes equations, therefore, the computational cost is lower than using the DNS and LES models. Thus, the RANS models are largely used to simulate turbulent flux in several areas and in complex problems simulations of the industry, an ideal tool to system design, optimizations, or even for cases when it is unfeasible to be done in lab, among others practical applications.

The RANS application consists in approximate the Reynolds stress terms to the RANS equations, resulting in different turbulence models to these terms. The eddy viscosity model (EVM) and Reynolds stress model (RSM) are the most used turbulence models. Among the EVM models, it can be mentioned the standard $k-\epsilon$ model (SKE), the renormalization group $k-\epsilon$ model (RNG), the realizable $k-\epsilon$ model (RKE) and the shear stress transport $k-\omega$ model (SST), and all of them are two equations eddy viscosity models. They have the Reynolds stress terms expressed by the eddy viscosity μ_t. The turbulent viscosity is based on the solutions of the equations for turbulent kinetic energy (k) and specific dissipation rate (ω) or turbulent dissipation rate (ϵ). These two-equations models has the advantage of computational efficiency, but the accuracy is limited by the hypothesis of isotropic eddy viscosity.

The SKE model was used in the simulated cases. In this model, the eddy viscosity is given by Eq. (6), while the velocity scale and the dissipation rate are presented respectively by the Eq. (7) and Eq. (8). These terms, after derived from the conservation equations and done some drastic simplifications, are transformed in the final equations in the form of $k-$ "$equation$" and turbulent dissipation ϵ, given by the Eq. (9) and Eq. (8), respectively. These two equations example why the SKE model is a two-equation model.

$$\mu_t = \rho C_\mu \frac{k^2}{\epsilon} \tag{6}$$

$$q = k^{1/2} \tag{7}$$

$$\epsilon \approx \frac{k^{3/2}}{l} \tag{8}$$

$$\frac{\partial(\rho k)}{\partial t} + \nabla\cdot(\rho k U_i) = \nabla\cdot\left[\frac{\mu_t}{\sigma_k}\nabla k\right] + 2\mu_t E_{ij}E_{ij} - \rho\epsilon \tag{9}$$

$$\frac{\partial(\rho\epsilon)}{\partial t} + \nabla\cdot(\rho\epsilon U_i) = \nabla\cdot\left[\frac{\mu_t}{\sigma_\epsilon}\nabla\epsilon\right] + C_{1\epsilon}\frac{\epsilon}{k}2\mu_t E_{ij}E_{ij} - C_{2\epsilon}\rho\frac{\epsilon^2}{k} \tag{10}$$

where:
U_i represents the velocity component in corresponding direction,
E_{ij} represents the component of deformation rate,
l represents the turbulent length scale.

2.2 The mesh development

The simulated case has a mesh designed based on the ejector model analyzed by García del Valle *et al.* (2015), which describes its dimensions. The ejector has a cylindrical design, the reason why it can be simulated using a symmetrical mesh, in other words, instead of using the entire cylinder, just a part of it is used. In this case this part has a small angle of $1°$, which reduces the mesh size in 359 times. In addition, the symmetrical mesh enables the mesh to be used just as a 2-D model, instead of the conventional 3-D. All these simplifications decrease both CPU time and use of RAM memory, which usually give faster and more accurate results. Using the blockMesh utility from OpenFOAM, the cells division must be done in a non-uniform quadrangular shape, because the blockMesh requires that some split lines must be kept to a perfect cell nodes connection, which is presented by the Fig. 2a.

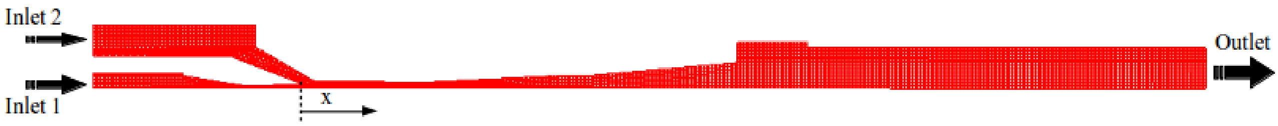

(a) 2-D mesh along the ejector

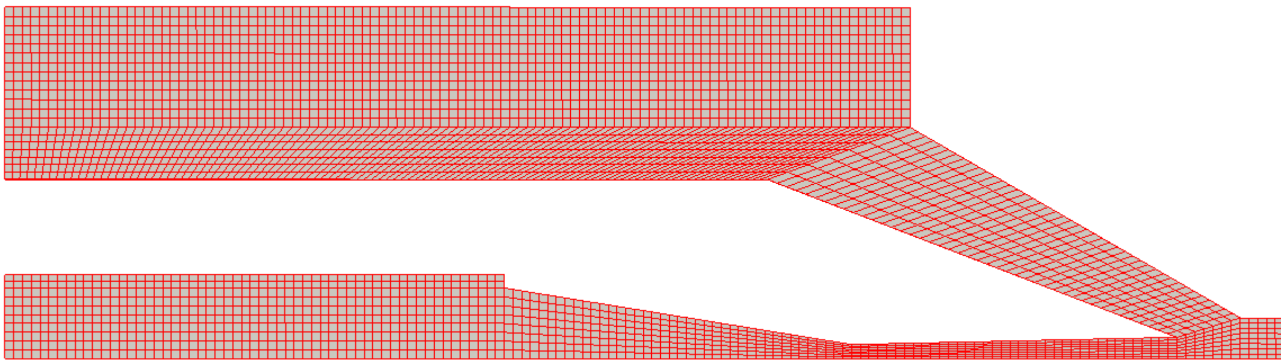

(b) Amplified mesh

Figure 2: The mesh used in the validation model

Initially the mesh was created with 11 thousand cells, whose number is convenient to simulate the desired cases in a suitable time, according to the practical tests. To assess the model consistency others mesh with different cells number are simulated and analyzed, as those with 5.500, 22.000 and 44.000 cells, which are split uniformly. An optimized mesh with 21.000 cells, which has a better refinement in the shock waves and supersonic velocities area, was also used during the analysis.

2.3 The solvers and the boundary conditions used

The native OpenFOAM solvers used during the simulation are the sonicFoam, rhoCentralFoam and rhoPimpleFoam, which succeed in the goal of this present work and the simulation characteristics, like the trans/supersonic speed regime and compressible fluid. In addition, the solver modFoam was developed based on sonicFoam to achieve more accurate results, including the Peng-Robinson equation in the numerical solver. To approximate the computational solution with the lab one, the Peng-Robinson equation can be used to better predict the gas behavior inside the ejector. This equation can achieve a good precision near the critical point of gases, mainly compared with the compressibility factor and liquid density. In this way, for critical situations, with high pressure and high temperature, this model is better than using the perfect gas hypothesis, and it will be analyzed in this work.

In the solver sonicFoam the total energy conservation calculation is significantly more accurate compared to the calculation of just thermal energy conservation. The sonicFoam energy calculus is done in terms of internal energy (or specific internal energy $\hat{u}$), like presented by the Eq. (11), however, the OpenFOAM allows the use of Peng-Robinson equation just when the energy is calculated in terms of enthalpy (or specific enthalpy $\hat{h}$), which restricts the solver sonicFoam. To bypass this problem, a new solver called *modFoam* was created based on sonicFoam, with the single modification in the energy equation that enables its calculation in terms of enthalpy, as presented by the Eq. (12). The new solver, therefore, is able to work with the same conditions as the sonicFoam, but with the Peng-Robinson equation enabled, which enables also the input of polynomials terms of enthalpy (h), thermal conductivity (κ) and dynamic viscosity (μ).

$$\frac{\partial}{\partial t}(\rho\hat{u}) + \nabla\cdot[\rho\mathbf{U}\hat{u}] = -\nabla\cdot\dot{q}_s - p\nabla\cdot\mathbf{U} + (\tau:\nabla\mathbf{U}) + \dot{q}_V \tag{11}$$

$$\frac{\partial}{\partial t}(\rho\hat{h}) + \nabla\cdot[\rho\mathbf{U}\hat{h}] = -\nabla\cdot\dot{q}_s + \frac{Dp}{Dt} + (\tau:\nabla\mathbf{U}) + \dot{q}_V \tag{12}$$

Each one of the four solvers described above are analyzed with the 11.000 cells initial mesh and just those who gave stability and convergence were approved, in other words, those who could keep the simulation running for long period without errors or crash, but with consistent results according to the applied physics. After these criteria were fulfilled, the cases were simulated until the inlets mass flux hit the same value as the outlet mass flux, which characterize the steady state. This last analysis become a requirement because the used solvers calculation was done for the transient flow instead of steady state.

Unfortunately the rhoPimpleFoam, despite some initials claims of use, could not be used in these cases because it does not fulfill the required criteria mentioned, even after the application of various different boundary conditions. The simulations using the solver rhoCentralFoam with the approved required criteria are set with the boundary conditions shown by the Tab. 1. The thermo-physical properties for the simulations using the perfect gas model can be followed in the Tab. 2, while the used values are those presented by the Tab. 3, where the M_m is the molar mass, Cp is the specific heat at constant pressure and Pr is the Prandtl number.

Table 1: Boundary conditions in the initial case using the rhoCentralFoam, sonicFoam or modFoam.

Property	Zone	rhoCentralFoam	sonicFoam or modFoam
p	Inlet 1	totalPressure	totalPressure
	Inlet 2	totalPressure	totalPressure
	Outlet	fixedValue	waveTransmissive
	Nozzle Wall	zeroGradient	zeroGradient
	Ejector Wall	zeroGradient	zeroGradient
U	Inlet 1	pressureInletOutletVelocity	pressureInletOutletVelocity
	Inlet 2	pressureInletVelocity	pressureInletVelocity
	Outlet	zeroGradient	zeroGradient
	Nozzle Wall	slip	noSlip
	Ejector Wall	slip	noSlip
T	Inlet 1	fixedValue	fixedValue
	Inlet 2	fixedValue	fixedValue
	Outlet	zeroGradient	zeroGradient
	Nozzle Wall	zeroGradient	zeroGradient
	Ejector Wall	zeroGradient	zeroGradient

Table 2: Overview of the thermo-physical properties with different gas equations.

	Type of Gas Equation	
thermoType entry	Perfect Gas Eq.	Peng-Robinson Eq.
type	hePsiThermo	hePsiThermo
mixture	pureMixture	pureMixture
transport	const	polynomial
thermo	hConst	hPolynomial
equationOfState	perfectGas	PengRobinsonGas
specie	specie	specie
energy	sensibleInternalEnergy	sensibleEnthalpy

The boundary conditions used with sonicFoam, as well as the thermo-physical properties are presented by the Tab. 1 and Tab. 2, respectively. The property values, shown by the Tab. 3, are the same as those for the rhoCentralFoam case because both use the perfect gas equation.

Table 3: Physical properties using the perfect gas equation at T = 300 K and p = $6,50$ bar.

Type	Property	Value
Mass	M_m	$102,03$ kg/kmol
Thermodynamics	Cp	1010 J/(kg.K)
Transport	μ	$11,8.10^-6$ Pa.s
	Pr	$0,857$

The boundary conditions in the walls, inlets and outlet of the ejector using the modFoam were the same as the sonicFoam, in other words, they are the same as presented in the Tab. 1. The thermo-physical properties, however, were different because of the modifications in the equation of state and it was solved by the Peng-Robinson equation, as well as the polynomial terms of some variables, according to the Tab. 2, where $CpCoeffs*$ are the 8 polynomial coefficients of the specific heat at constant pressure, $\mu Coeffs*$ are the 8 polynomial coefficients of the dynamic viscosity, $\kappa Coeffs*$ are the 8 polynomial coefficients of the thermal conductivity, Tc is the critical temperature, Vc is the critical volume, Pc is the critical pressure and AF is the acentric factor.

Note: the 8 polynomial coefficients are in the form of "(a0 a1 a2 a3 a4 a5 a6 a7)", which represents: $a0 + a1.x + a2.x^2 + a3.x^3 + a4.x^4 + a5.x^5 + a6.x^6 + a7.x^7$.

The simulations using the modFoam solver were done in two steps to keep the criteria of convergence and stability: firstly the case was simulated using the Peng-Robinson equation and the terms with constant coefficients. This was specified in the thermo-physical properties, in which the polynomial terms was kept equal to zero, as referred in the Tab. 4. After the mass flux stabilization the simulation was modified in the terms values from these polynomial properties, keeping as presented by the Tab. 5. Next the simulation ran the same way the others solvers until the mass flux equalization to achieve the final results.

Table 4: Physical properties using the Peng-Robinson equation with constant coefficients at T = 300 K and p = $6,50$ bar.

Type	Property	Value
Mass	M_m	$102,03$ kg/kmol
Thermodynamics	$CpCoeffs$	1010 0 0 0 0 0 0 0 J/(kg.K)
Transport	$\mu Coeffs$	$11,8.10^-6$ 0 0 0 0 0 0 0 Pa.s
	$\kappa Coeffs$	$0,0139$ 0 0 0 0 0 0 0 W/(m.K)
Equation of State	Tc	$374,23$ K
	Vc	$0,19944$ m^3/kmol
	Pc	4059280 Pa
	AF	$0,32684$

Table 5: Physical properties using the Peng-Robinson equation with polynomial coefficients at T = 300 K and p = $6,50$ bar.

Type	Property	Value
Mass	M_m	$102,03$ kg/kmol
Thermodynamics	$CpCoeffs$	$6,817209.10^7$ $-1,481880.10^6$ $1,374912.10^4$ $-7,048492.10^1$ $2,156538.10^{-1}$ $-3,938422.10^{-4}$ $3,975915.10^{-7}$ $-1,711858.10^{-10}$ J/(kg.K)
Transport	$\mu Coeffs$	$-2,008112$ $4,667447.10^{-2}$ $-4,635735.10^{-4}$ $2,550423.10^{-6}$ $-8,394360.10^{-9}$ $1,652916.10^{-11}$ $-1,802965.10^{-14}$ $8,404350.10^{-18}$ Pa.s
	$\kappa Coeffs$	$-1,835270.10^4$ $4,259630.10^2$ $-4,224370$ $2,320450.10^{-2}$ $-7,624800.10^{-5}$ $1,498770.10^{-7}$ $-1,631820.10^{-10}$ $7,591860.10^{-14}$ W/(m.K)
Equation of State	Tc	$374,23$ K
	Vc	$0,19944$ m^3/kmol
	Pc	4059280 Pa
	AF	$0,32684$

3. RESULTS AND DISCUSSION

The most relevant items analyzed in this section were the results validation compared to the lab experiments, the simulation accuracy analysis and if it will be possible to use this model test to perform a numerical study. Remember that the used mesh was identical between all the solvers tested, in other words, it had initially 11 thousand cells to analyze the stability and convergence criteria of the simulation, and after the mesh was changed to 5.500, 22.000, 44.000 and 21.000 cells according to the possibility and the requirement of more accurate results. Some mesh examples are presented by the Fig. 4 and Fig. 3, which describes the Mach number and the pressure along the ejector during the simulations.

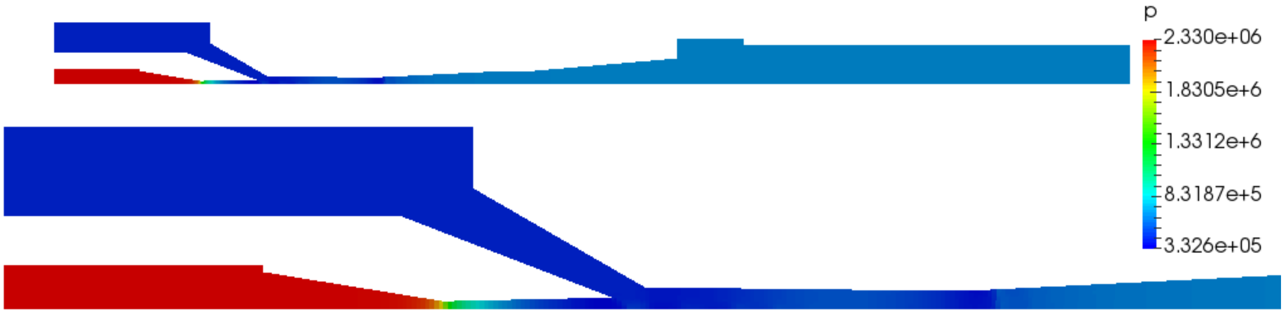

Figure 3: The pressure variation in the analyzed model with 11.000 cells

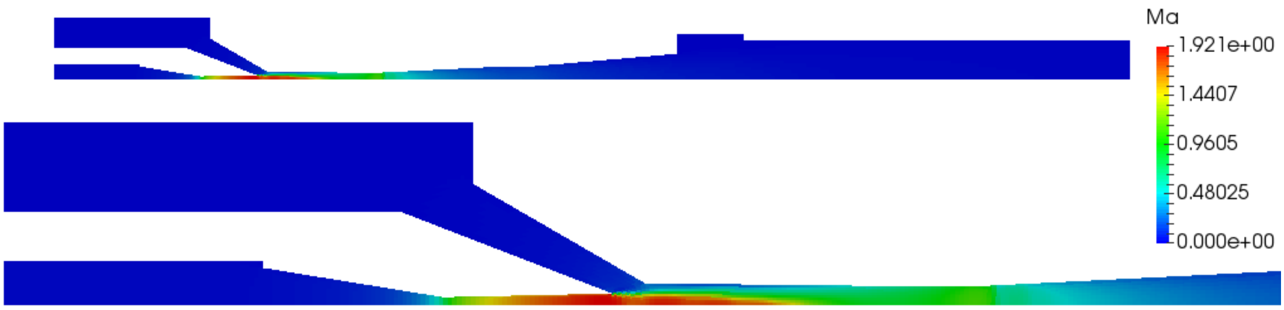

Figure 4: The Mach number variation in the analyzed model with 11.000 cells

The big advantage about using the rhoCentralFoam was the ease to apply it in the studied case and the simplicity compared to the sonicFoam, however it could disrupt negatively the results precision and convergence. Despite the simulation theoretically did not express the ejector physics correctly because of the supersonic velocity effects that arise in the nozzle, it was a great solver for the first tests. After some boundary condition tests, some simulations were taken as stable, however, the high CPU time requirement inhibited the complete simulation execution with the initial mesh of 11 thousand cells, even if this number were decreased by half.

The solver who gave the most consistent and stable results without high CPU time requirement was the sonicFoam. This specific solver for trans/supersonic simulations was enough to validate the model without the application of Peng-Robinson equation. The sonicFoam was used heavily since the results were achieved quicker than any other standard solver used. Various simulations were done and the ER results are summarized in the Tab. 6, which also contains the modFoam results. The error found in sonicFoam ER simulation are quite good using the initial mesh of 11.000 cells, however, this error increased by 5% when the mesh was refined by two times. At the moment this effect does not have an explanation and the investigation about the main causes are in progress. Despite this problem, the error found using the initial mesh was a reasonable value for this case.

The Fig. 5 presents the results in relation to the lab wall pressure measurements and the x-axis distance is specified in the 2a. The wall pressure along the ejector had a difference compared to the lab results and it was due to the perfect gas hypothesis applied on sonicFoam, which changed the reached pressure and also its peak location. It can be observed that the wall pressure do not changed according to the mesh refinement level.

The modified solver made to apply the Peng-Robinson equation, the modFoam, performed in a similar way than sonicFoam, with stability in the same boundary conditions and similar convergence. The comparison between the ER results can be followed by the Tab. 6, and resulted in an error higher than using the sonicFoam, as well as the increasing of this error while the mesh was refined. These effects do not have an explanation now, but some researches and analyses are done to find why it occurs.

The wall pressure profile comparison using the modFoam solver is presented in the Fig. 6. The pressure profile, as expected, were better than using the perfect gas model, mainly in the 22.000 cells results. The pressure along the ejector

Table 6: sonicFoam and modFoam results for the case 1.

	sonicFoam		modFoam(1)		modFoam(2)	
Mesh Cells Number	ER	Error [%]	ER	Error [%]	ER	Error [%]
Lab experiment	0,592	-	-	-	-	-
5.500	0,665	12%	-	-	-	-
11.000	0,691	17%	0,643	9%	0,741	25%
22.000	0,723	22%	0,669	13%	0,77	30%
21.000 opt.	0,718	21%	-	-	-	-

(1) is the modFoam simulation 1st step
(2) is the modFoam simulation final step

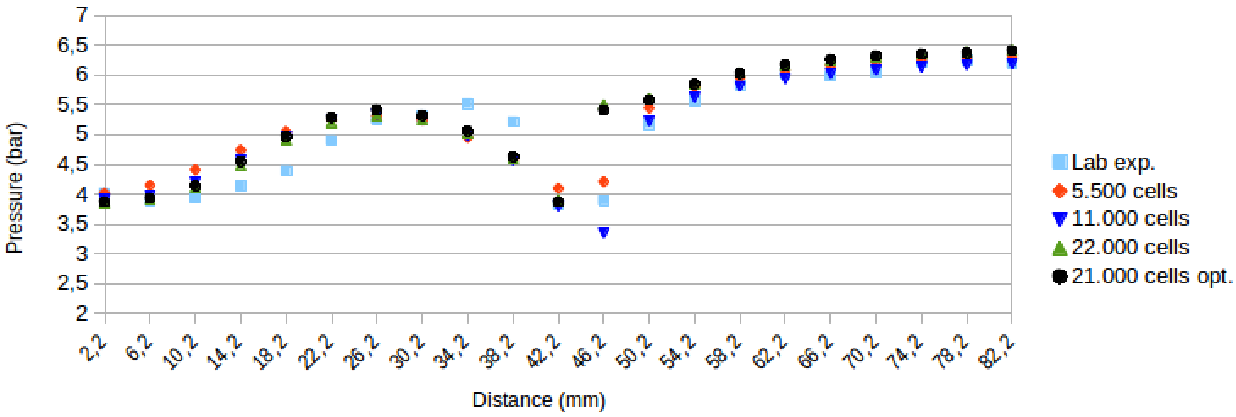

Figure 5: Pressure graph along the ejector wall using the sonicFoam

using this mesh was similar than that found in lab experiments, which describes that the CFD simulation can reach some good results as the lab does.

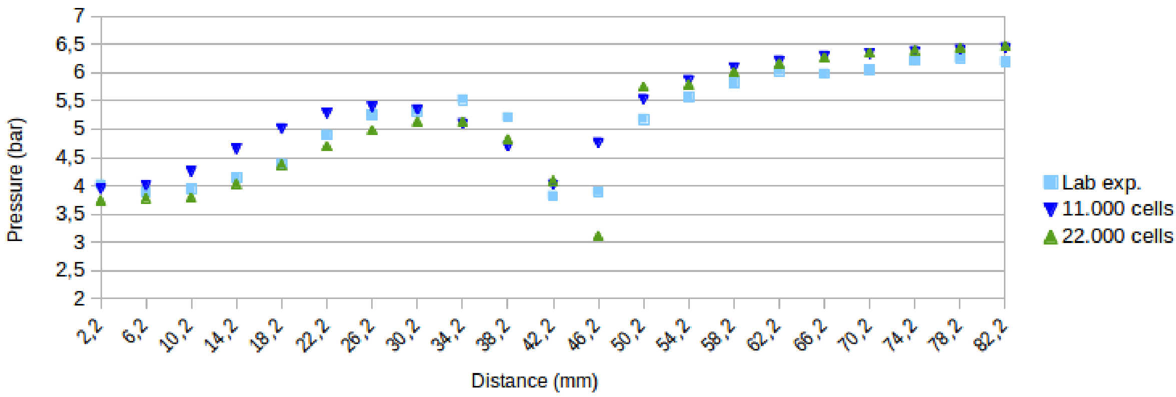

Figure 6: Pressure graph along the ejector x axis using the modFoam

4. CONCLUSION

The cases simulated with the rhoCentralFoam were not performed until the end because the very high CPU time requirement, which excluded this solver from being used in this work. The sonicFoam and modFoam simulations were performed relatively well and the ER results were near the lab experiments, however, as far as the mesh was refined, the error related to the lab results increased. Until this moment this effect cannot be explained and some researches are being developed to find the causes.

A comparison between the sonicFoam and modFoam in relation to the wall pressure profile showed a better pressure prediction of the Peng-Robinson equation compared to the perfect gas equation. The use of modFoam was essential to keep the pressure profile near the lab results.

5. ACKNOWLEDGEMENTS

This work is supported by CAPES, which granted the scholarship to the research. This research was supported by resources supplied by the Center for Scientific Computing (NCC/GridUNESP) of the São Paulo State University (UNESP).

6. REFERENCES

Abed, A.M., Alghoul, M. and Sopian, K., 2016. "Performance evaluation of flash tank-absorption cooling cycle using two ejectors". *Applied Thermal Engineering*, Vol. 101, pp. 47–60. ISSN 13594311. doi:10.1016/j.applthermaleng.2016.02.074. URL `http://linkinghub.elsevier.com/retrieve/pii/S1359431116302174`.

Ablwaifa, A.E., 2006. *A Theoretical and Experimental Investigation of Jet-Pump Refrigeration system*. Ph.D., School of the Built Environment, University of Nottingham, Nottingham, UK. URL `http://eprints.nottingham.ac.uk/11746/1/429928.pdf`.

Allouche, Y., Bouden, C. and Varga, S., 2014. "A CFD analysis of the flow structure inside a steam ejector to identify the suitable experimental operating conditions for a solar-driven refrigeration system". *International Journal of Refrigeration*, Vol. 39, pp. 186–195. ISSN 01407007. doi:10.1016/j.ijrefrig.2013.07.027. URL `http://linkinghub.elsevier.com/retrieve/pii/S0140700713002144`.

Bartosiewicz, Y., Aidoun, Z., Desevaux, P. and Mercadier, Y., 2005. "Numerical and experimental investigations on supersonic ejectors". *International Journal of Heat and Fluid Flow*, Vol. 26, No. 1, pp. 56–70. ISSN 0142727X. doi:10.1016/j.ijheatfluidflow.2004.07.003. URL `http://linkinghub.elsevier.com/retrieve/pii/S0142727X04001158`.

Cardemil, J.M. and Colle, S., 2012. "A general model for evaluation of vapor ejectors performance for application in refrigeration". *Energy Conversion and Management*, Vol. 64, pp. 79–86. ISSN 01968904. doi:10.1016/j.enconman.2012.05.009. URL `http://linkinghub.elsevier.com/retrieve/pii/S0196890412002154`.

Chen, J., Jarall, S., Havtun, H. and Palm, B., 2015. "A review on versatile ejector applications in refrigeration systems". *Renewable and Sustainable Energy Reviews*, Vol. 49, pp. 67–90. ISSN 13640321. doi:10.1016/j.rser.2015.04.073. URL `http://linkinghub.elsevier.com/retrieve/pii/S1364032115003433`.

García del Valle, J., Saíz Jabardo, J., Castro Ruiz, F. and San José Alonso, J., 2014. "An experimental investigation of a R-134a ejector refrigeration system". *International Journal of Refrigeration*, Vol. 46, pp. 105–113. ISSN 01407007. doi:10.1016/j.ijrefrig.2014.05.028. URL `http://linkinghub.elsevier.com/retrieve/pii/S0140700714001406`.

García del Valle, J., Sierra-Pallares, J., Garcia Carrascal, P. and Castro Ruiz, F., 2015. "An experimental and computational study of the flow pattern in a refrigerant ejector. Validation of turbulence models and real-gas effects". *Applied Thermal Engineering*, Vol. 89, pp. 795–811. ISSN 13594311. doi:10.1016/j.applthermaleng.2015.06.064. URL `http://linkinghub.elsevier.com/retrieve/pii/S1359431115006237`.

Hakkaki-Fard, A., Aidoun, Z. and Ouzzane, M., 2015. "A computational methodology for ejector design and performance maximisation". *Energy Conversion and Management*, Vol. 105, pp. 1291–1302. ISSN 01968904. doi:10.1016/j.enconman.2015.08.070. URL `http://linkinghub.elsevier.com/retrieve/pii/S0196890415008249`.

Versteeg, H.K. and Malalasekera, W., 2007. *An Introduction to Computational Fluid Dynamics*. Pearson Education, Ltd., India, 2nd edition. ISBN 978-81-317-2048-6.

Yen, R., Huang, B., Chen, C., Shiu, T., Cheng, C., Chen, S. and Shestopalov, K., 2013. "Performance optimization for a variable throat ejector in a solar refrigeration system". *International Journal of Refrigeration*, Vol. 36, No. 5, pp. 1512–1520. ISSN 01407007. doi:10.1016/j.ijrefrig.2013.04.005. URL `http://linkinghub.elsevier.com/retrieve/pii/S0140700713000820`.

Zikanov, O., 2010. *Essential Computational Fluid Dynamics*. Wiley-India, India, 1st edition. ISBN 978-81-265-3497-5.

7. RESPONSIBILITY NOTICE

The authors are the only responsible for the printed material included in this paper.